Effects of Motion Cueing on Curve Driving

Herman J. Damveld [1,2], Mark Wentink [3], Peter M. van Leeuwen [2], Riender Happee [2]
(1) Delft University of Technology, Faculty of Aerospace Engineering, E-mail: H.J.Damveld@tudelft.nl
(2) Delft University of Technology, Faculty of Mechanical, Maritime and Materials Engineering, E-mail: P.M.vanLeeuwen@tudelft.nl, R.Happee@tudelft.nl
(3) Desdemona B.V., E-mail: Mark.Wentink@desdemona.eu

Abstract *– A curve negotiation task at a prescribed and constant velocity was performed in the presence of external disturbances. The driver's goal was to simultaneously minimize the heading error and lateral position error. The present paper investigates the separate contributions of the road tracking and the disturbance to the heading and position errors, and more important, the effect of motion on these contributions. Four different motion cueing conditions were tested: 1) rumble only, 2) one-to-one yaw, 3) centrifuge with onset yaw, and 4) lateral track with onset yaw. It was concluded that none of the motion cueing conditions had a significant or large effect on the performance or control activity.*

Key words: *curve driving, motion cueing, target tracking, disturbance rejection*

Introduction

In the DRIVOBS project we are developing methods to obtain objective measures representing many aspects of the driver's behavior. Besides using physiological measures, such as heart rate variability or gaze tracking, the driver's behavior can be objectively quantified using system identification and parameter estimation (SIPE) to obtain driver models, both in real cars and in driving simulators. The objectively obtained driver behaviour observations enable industry to gain insight into the effect of several car driving aspects, such as proposed changes to the vehicle dynamics and steering systems. Furthermore such observations can objectively quantify effects of driving simulator configurations, such as the motion cueing system.

System identification methods have been used extensively to identify pilot models while controlling aircraft dynamics [Dam1, Poo1]. The current state of the art allows us to simultaneously identify the separate contributions of the pilot's visual system, the vestibular system and the neuromuscular system [Dam2, Dam3]. System identification was also used successfully to observe changes in the estimated pilot model parameters due to changes in the motion cueing algorithm [Zaa1].

Contrary to the displays used in aircraft control, the visual view in car driving has a rich optical flow, which provides the driver with a good perception of motion [Gib1]. In addition, aircraft displays usually only show an error between a commanded and a tracking symbol, allowing the pilot only to respond to the error, while the typical outside visual in car driving allows the driver to anticipate the future road geometry due to the presence of preview information.

Due to the strong visual cues and the possibility to anticipate it should be questioned whether the addition of motion cues in driving simulators will affect the drivers' control behaviour and performance. This was studied previously by others. For instance in [Val1], significant effects of the cueing algorithm were found in a city drive task using subjective rating scales, but objective measures did not reveal significant effects.

Obviously the effects of motion strongly depend on the task at hand. In a common curve negotiation task, a driver has to perform a combined target following and disturbance rejection task. The target consists of the road geometry, which simultaneously prescribes the car's heading and lateral position. The disturbance can stem from wind or road irregularities, which normally cannot be anticipated.

The goal of the present study is to objectively investigate the effects of several different motion cueing solutions on the human steering behaviour during curve driving in the presence of disturbances. We used the Desdemona simulator to test four different motion cueing algorithms. The experiment was designed to enable system identification and parameter estimation of the driver model. The used design also allows to differentiate between the target following and disturbance rejection effects. The present paper will only focus on those results.

Background

Driver models

A car driver perceives and processes information through a number of systems, including the visual system, the vestibular system and the neuromuscular system. Driver models in path following have traditionally focused on the use of visual information. Several published models realistically capture driving behavior but many models are unsuitable for system identification [Ste1]. The present study is based on the visual driver model derived by Allen and McRuer [All1, McR1]. A slightly adapted model structure is shown in Figure 1. This model is based on the assumption that the human driver is capable of perceiving three signals, the commanded heading ψ_c, the heading angle error ψ, and the lateral position error y (with respect to the center of the lane). The output of the driver is the steering wheel angle δ_s, which is based on a linear, time-invariant function of the inputs, and the remnant n. This remnant represents possible time-varying and non-linear effects. The remnant is usually small compared to the linear contribution and is usually neglected.

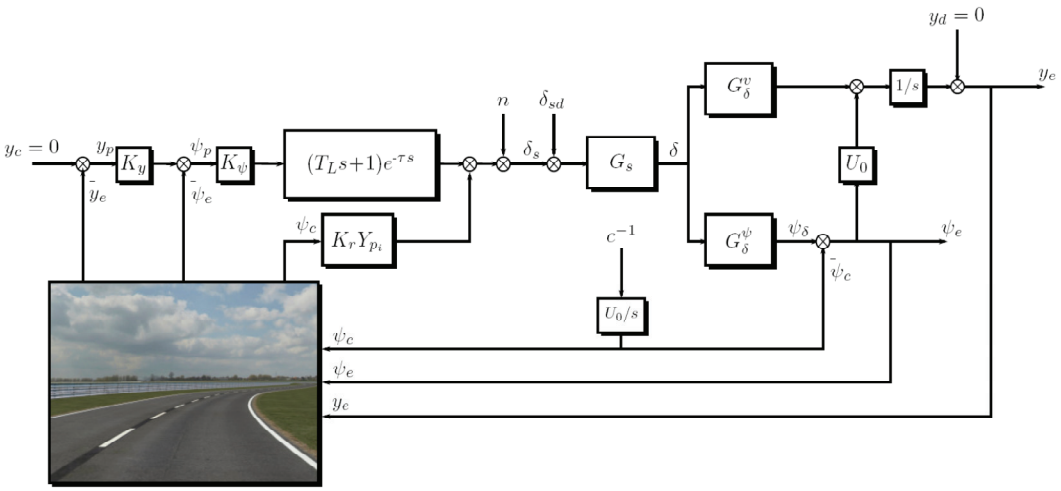

Figure 1. Driver vehicle model for control of road curvature and random disturbances.

Table 1. Description of signals and parameters in the driver-vehicle model.

Signals:

ψ_c	commanded heading
ψ_e	visible heading error
ψ_p	internal heading error incl. lateral error contribution
ψ_δ	car heading
y_c	commanded lateral deviation (= 0)
y_e	visible lateral position error
y_p	internal lateral position error
y_d	lateral position disturbance
n	remnant
δ_s	steering wheel angle
δ_{sd}	steering wheel disturbance
δ	front wheel angle
c	commanded curvature

Driver model parameters:

K_y	lateral position feedback gain
K_r	feedforward gain
K_ψ	heading feedback gain
T_L	lead time constant
τ	time delay
Y_{p_i}	feedforward control dynamics

Car model transfer functions:

G_s	steering wheel to front wheel ratio
G_δ^v	lateral velocity due to front wheel angle
G_δ^ψ	heading due to front wheel angle
U_0	car velocity (constant)

Target Following and Disturbance Rejection

In the curve negotiation task studied, a driver has to perform a combined target following and disturbance rejection task, and his goal is to simultaneously minimize the heading error and lateral position error of the vehicle by turning the steering wheel.

The target is provided as the commanded heading ψ_c, while the wind or road disturbance is simulated by a steering wheel disturbance δ_{sd} which is added to the driver's steering wheel angle before entering the vehicle model. The disturbance does not result in physical steering wheel forces or rotations.

Both target and disturbance signals will result in heading and lateral position errors. The present paper will investigate the separate contributions of the target and the disturbance to the heading and position errors, and more important, the effect of motion on these contributions.

In a situation *without motion*, the driver uses two visual feedback paths (operating on y_e and ψ_e) and one visual feedforward path (operating on ψ_c, see Figure 1). The heading and lateral position feedback paths allow the driver to respond to errors due to the commanded road heading and due to disturbances.

The visual feedforward path allows the driver to respond directly to the commanded heading. The driver can adapt his control behaviour to invert the vehicle dynamics, and as a result the heading and lateral position errors will become very small [Was1]. The visual feedforward path will have no effect on the mitigation of disturbances. These and residual target tracking errors will have to be minimized by the visual feedback paths.

When *motion is added*, the human driver will perceive vestibular information as well, which provides information about the change of the heading ($\dot{\psi}$) and position ($\ddot{y}$) of the vehicle. This allows the driver to respond to both disturbance and target signals. There is one important difference between the motion cues due to the target and disturbance signals: the motion cues due to the target following task are only the result of the drivers own steering actions, while the cues due to the disturbance rejection task are caused by the driver's own steering actions and the steering wheel disturbance. For this reason, the expected main effect of the addition of motion is an increase of the disturbance rejection performance. This was indeed demonstrated by [Zaa2] in an aircraft pitch control task without a preview display.

Method

Two uncorrelated forcing functions were designed in order to be able to distinguish between the effects of motion on the performance contributions of the target tracking task and the disturbance rejection task. Each of the forcing functions was composed of N sinusoids:

$$i(a) = \sum_{j=1}^{N} A_j \sin\left(\omega_j a + \varphi_j\right) \tag{1}$$

With:

i forcing function,

a along track distance,

A_j amplitude of sinusoid j,

ω_j frequency of sinusoid j, and

φ_j phase of sinusoid j.

Both forcing functions were designed as a function of the along track distance, which is the distance measured along the centreline of the lane. Consequently, the frequencies ω_j are spatial frequencies, meaning that both forcing functions are periodic across position in space instead of time.

The frequencies in the target forcing function ψ_c and the disturbance forcing function δ_{sd} are mutually exclusive, which allows us to separate their contributions in the frequency domain. The amplitudes and phases of the forcing functions were selected to result in quasi-random road curves and disturbances [Dam4].

A number of drivers performed the combined tracking and disturbance task several times, during which the heading error $\psi(t)$, the lateral position error $y(t)$ and the steering wheel angle $\delta_s(t)$ were recorded as a function of time. Using cubic interpolation, these recording were transformed from the time domain to the spatial domain as a function of the along track distance a. For example, the transformation for the steering wheel angle is:

$$\delta_s(t) \rightarrow \delta_s(a) \tag{2}$$

The spatial domain data were then transformed to the spatial frequency domain using a Fourier transformation. The Fourier transformed steering wheel angle is:

$$\Delta_s(\omega) = \int_{-\infty}^{\infty} \delta_s(a)\, e^{-j\omega a} da \tag{3}$$

The Fourier transformed data can now be averaged over the repetitions per subject and per condition to reduce the remnant.

The total variance, usually called *power*, of the steering wheel angle is a measure of the control activity, and can be calculated from the Fourier transformed data:

$$\sigma_{\delta_s}^2 = \frac{1}{\pi} \int_0^{\infty} \Phi_{\delta_s \delta_s}(\omega) d\omega \tag{4}$$

in which ω is the spatial frequency, and $\Phi_{\delta_s\delta_s}$ is the (auto) power spectral density of δ_s, here approximated by the periodogram:

$$\Phi_{\delta_s\delta_s}(\omega) = \frac{da}{N_s}\,\overline{\Delta_s(\omega)}\,\Delta_s(\omega) \tag{5}$$

With:

da the sampling interval in meters,

N_s the number of samples in δ_s, and

Δ_s the Fourier transform of δ_s.

Since the target and disturbance forcing functions contain power at distinct frequencies, the amount of power in the steering wheel angle signal caused by each forcing function can be calculated separately by integrating only over the frequencies in each forcing function. For instance, the power in the steering wheel angle signal due to the commanded heading forcing function is:

$$\sigma^2_{\delta_{s\psi_c}} = \frac{1}{\pi}\int_{\omega_{\psi_c}} \Phi_{\delta_s\delta_s}(\omega)d\omega \tag{6}$$

And the power due to the disturbance forcing function can be calculated similarly. The power in the remnant can be approximated by integrating over all frequencies that are not in either forcing function.

In a similar way the variance of the heading error and the lateral position error can be calculated and broken down into components due to the commanded heading, the steering wheel disturbance, and the remnant.

Experiment

We performed an experiment to determine the control activity and tracking performance during a curve negotiation task in the presence of disturbances as shown in Figure 1. The effects of motion were tested using four different motion cueing algorithms, including a condition without task-related motion (rumble only). Five subjects in the age of 20 to 54 performed five repetitions per motion cueing condition. The last three repetitions per condition were averaged to calculate the dependent measures, which are the control activity, and the heading and lateral position tracking performance. These are broken down into the separate contributions of the target forcing function, disturbance forcing function and remnant.

Apparatus

The effects of motion were studied using the high-end motion-based Desdemona simulator [Wen1]. The Desdemona motion platform has six serial degrees-of-freedom, starting with a central yaw axis (centrifuge), a horizontal axis (8m), and a vertical axis (2m), then the cabin itself can rotate freely in roll, yaw and pitch (>360º). All axes can move independently of each other. The exterior is shown in Figure 2a.

The simulator cabin was equipped with a five beamer projection system. The three front beamers produced high resolution images at 1400x1050px, while the side projection had a resolution of 1024x768px. The steering wheel was positioned in the center of the cabin, and was configured to behave as a mass-spring-damper system.

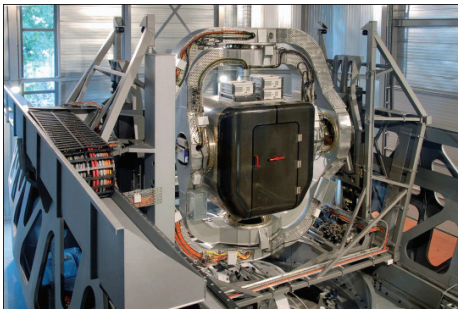

a. exterior

b. Interior

Figure 2. Desdemona motion system and cabin.

Forcing Functions

Both the commanded heading and steering wheel disturbance forcing function were composed of 10 sinusoids. To prevent subjects from learning the forcing functions by heart, we used different phase sets for both forcing functions in each repetition. The road length amounted to 1589.58m, of which 200m were used as lead-in distance, and 1389.58m were used for the actual calculations. The properties of one realization of the commanded heading

and the steering wheel disturbance are listed in Table 2, and the spatial domain signals are show in Figure 3. An impression of the road's characteristics is given in Figure 2b.

Table 2. Forcing function properties, one realization.

Commanded heading ψ_c			
Frequency (rad/m)	Frequency (rad/s)	Amplitude (rad)	Phase (rad)
0.0090	0.1256	0.5310	2.2365
0.0136	0.1884	0.3540	2.3982
0.0317	0.4396	0.1517	2.6802
0.0362	0.5024	0.1328	2.4867
0.0859	1.1932	0.0535	4.0601
0.0904	1.2560	0.0508	0.4553
0.2125	2.9516	0.0181	2.1519
0.2170	3.0144	0.0177	4.1765
0.4476	6.2172	0.0029	-0.0297
0.4522	6.2800	0.0029	-1.3858

Steering wheel disturbance δ_{sd}			
Frequency (rad/m)	Frequency (rad/s)	Amplitude (rad)	Phase (rad)
0.0181	0.2512	0.0361	0.3196
0.0226	0.3140	0.0361	1.5997
0.0407	0.5652	0.0361	-1.2249
0.0452	0.6280	0.0361	1.2446
0.0950	1.3188	0.0361	3.6996
0.0995	1.3816	0.0361	-0.8979
0.2216	3.0772	0.0361	-0.9907
0.2261	3.1400	0.0361	0.8396
0.4567	6.3428	0.0180	2.1313
0.4612	6.4045	0.0180	4.0572

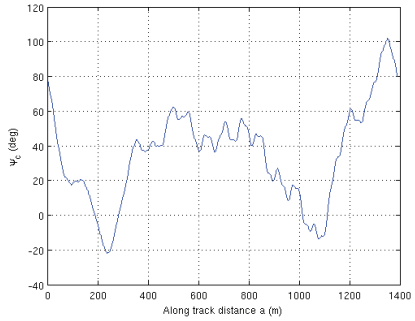

a. Commanded heading.

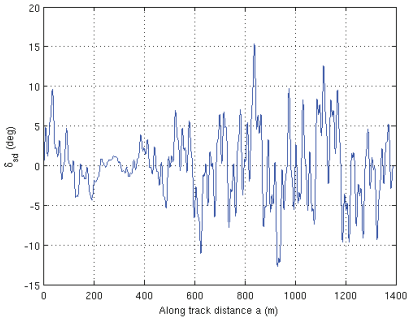

b. Steering wheel disturbance.

Figure 3. One realization of the forcing functions.

Car Model

A two degree-of-freedom car model was used [Rie1], which only describes the horizontal in-plane behaviour. The model uses the front wheel angle δ as an input and its outputs are the vehicle heading angle ψ_c and lateral velocity v. The car's position can be derived from the lateral velocity and heading angle. The vehicle's velocity was kept constant at 50 km/h.

Independent Variables

Four motion conditions were tested. Figure 4 depicts the motion cueing algorithms:

1. *Rumble only*: Only the vertical axis and cabin roll were used to simulate "road feel" contact between tyres and the road. The motion consisted of small amplitude white noise filtered by a low-pass filter, with a cut-off frequency and gain determined by the velocity of the car. Road rumble was also simulated in all other conditions.
2. *One-to-one yaw*: The cabin was positioned on-center, in the middle of the linear rail. The central yaw axis and the cabin yaw axis are then co-linear. High- and low-frequency yaw of the simulated car are divided over the central yaw and gimbal yaw axis, respectively, resulting in a one-to-one simulation of car yaw. In this solution, the accompanying lateral acceleration is not simulated.
3. *Centrifuge and onset yaw*: The cabin is positioned at the end of the linear track (R=4.0m). The central yaw spins the cabin around with 90º/s to produce a centrifugal force of 1g at R=4.0m. The resulting G-force felt by the subject is 1.4g. In addition, the subject is facing out from the center of centrifugation and is pitched 45º on his back, so that the resulting G-force is in the vertical direction again. In this position, the gimbal yaw axis is turned to tilt the centrifugal acceleration vector sideways to produce sustained lateral specific force. Due to the pitched position of the subject, part of this tilt-rotation is felt by the subject as yaw 'into the corner', coherent with the rotation of the simulated car driving through the corner. The part of the tilt-rotation that is felt as roll generates a false cue. The central yaw is used to generate sustained g-forces. The cabin yaw is used to align the centrifugal force with the lateral acceleration in the car. The heave and roll axis provide road rumble cues.

4. *Lateral track and onset yaw*: The horizontal track (R) is used to simulate lateral acceleration onsets (high-pass filtered car acceleration). The solution used about 6m of the horizontal track. Part of the sustained lateral specific force in corners is simulated applying moderate roll tilt (low-pass filtered, no rate limit applied). High-frequency yaw onsets are simulated by turning the yaw gimbal. In order to prevent misalignment of the simulated lateral acceleration the amplitude of the yaw gimbal movement is kept small.

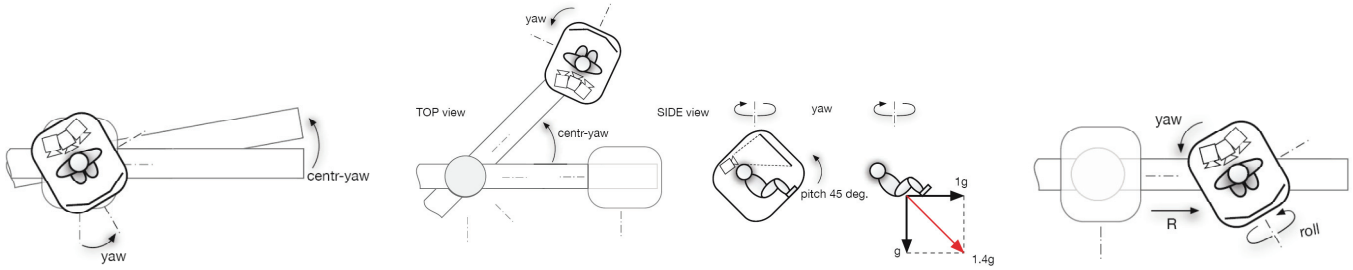

a. One-to-one yaw. **b. Centrifuge and onset yaw.** **c. Lateral track and onset yaw.**

Figure 4. Motion cueing conditions.

Dependent Measures

As discussed in the previous section, the dependent measures of interest are

1. the control activity, expressed by the variance of the steering wheel angle,
2. the heading tracking performance, expressed by the variance of the heading error, and
3. the lateral position tracking performance, expressed by the variance of the lateral position tracking error.

As explained in the Method section, the contributions of the target and disturbance forcing functions to the variances can be determined separately.

Results

Control Activity

Figure 5 shows the variance of the steering wheel angle, which is a measure for the driver's control activity. The gray bars indicate the subject means, averaged over three repetitions. The average over the subject means, which is the condition mean, is indicated by the closed circles. The error bars represent the 1-sigma standard deviation, corrected for between-subject effects.

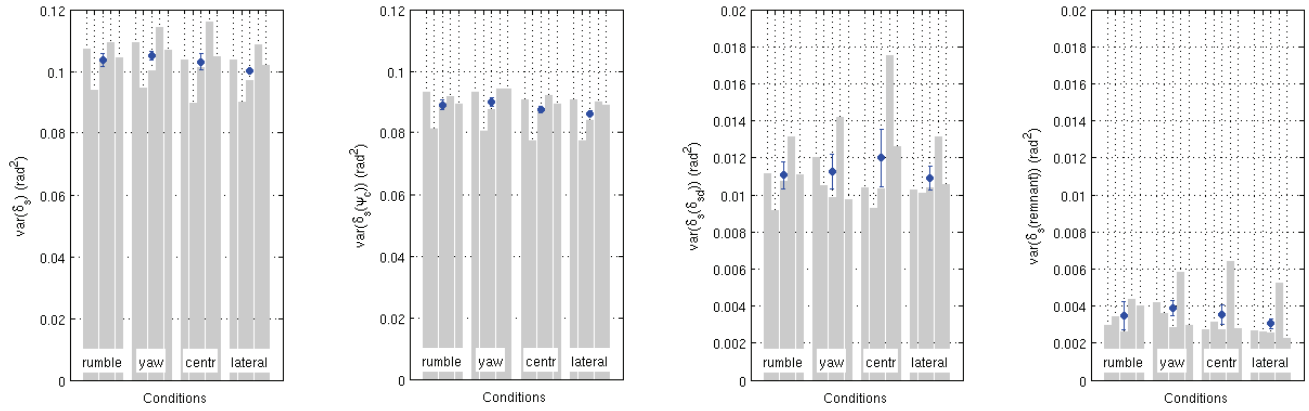

a. Total variance. **b. Variance due to target tracking.** **c. Variance due to disturbance rejection.** **d. Variance due to remnant.**

Figure 5. Control Activity.

The total variance shows little difference between the four conditions. Nevertheless, a repeated measures analysis of variance (ANOVA) indicates a significant effect of the motion condition on the control activity. Planned simple contrasts, comparing each condition to the rumble only condition, only revealed a significant difference between the rumble and lateral conditions.

An ANOVA of the variance contribution due to the commanded heading forcing function (Figure 5b) also indicated a significant, but small, effect of the motion condition. Planned contrasts showed that the control activity was significantly lower during the lateral condition compared to the rumble only condition. Figure 5c and d did not contain any significant differences.

Heading Tracking Performance

The main performance metric is the variance of the heading error, shown in Figure 6.

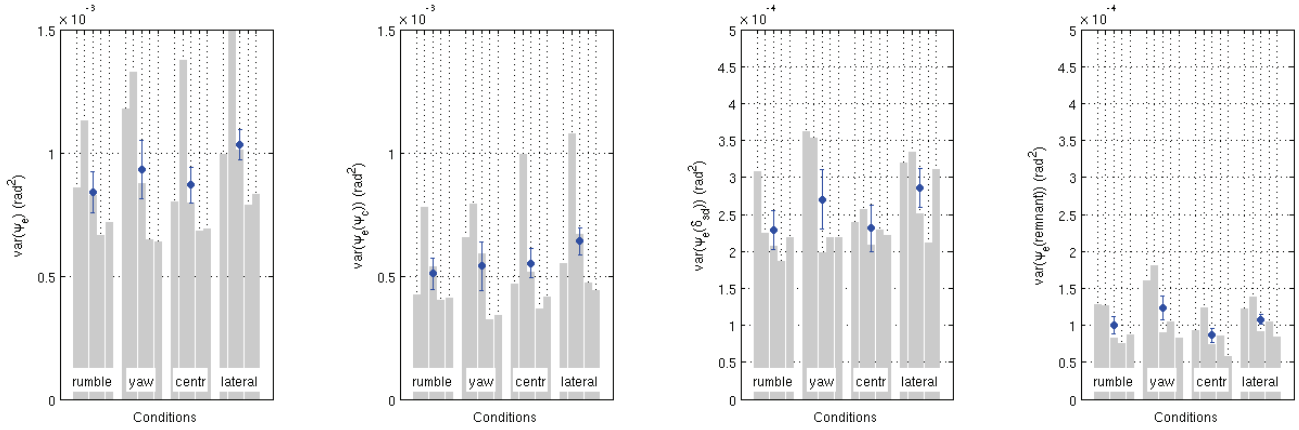

a. Total variance. **b. Variance due to target tracking.** **c. Variance due to disturbance rejection.** **d. Variance due to remnant.**

Figure 6. Heading tracking Performance.

The total variance does not show any improvements for the yaw, centrifuge or lateral conditions compared to the rumble only condition, and the performance in the yaw and lateral conditions seems even to have deteriorated by about 10-20%. An ANOVA confirms a significant effect of motion on the heading tracking performance, and planned contrasts reveal a significant performance deterioration, but only between the rumble and lateral conditions. It appears that this significant effect is caused by the combination of the contributions in Figure 6b, c and d, since the separate contributions are not significant.

Lateral Position Tracking Performance

The variance of the lateral position error is a metric for the positional tracking performance. The lateral position error is partly the result of the integrated heading error, hence similar results are expected.

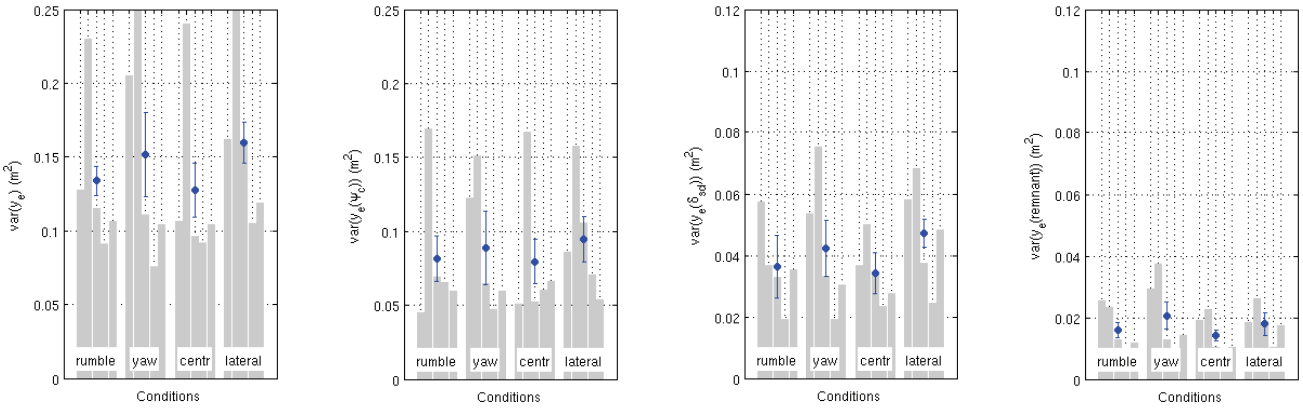

a. Total variance. **b. Variance due to target tracking.** **c. Variance due to disturbance rejection.** **d. Variance due to remnant.**

Figure 7. Lateral position tracking performance.

Although the lateral position performance appears to have decreased by about 13-19% in the yaw and lateral conditions, an ANOVA does not reveal any significant effect of motion. This is also the case for the separate contributions in Figure 7b, c and d.

Discussion

Based on previous work on motion cueing in aircraft pitch tracking tasks [Zaa1] it was expected to see an increase in the control activity when motion was added, both for the target tracking and disturbance rejection task. In the present study, a small decrease in control activity was seen, and only in the lateral motion condition for the target tracking task.

In addition, a heading tracking performance increase was expected, predominantly for the disturbance rejection task. In contrast we only found a very small performance decrease for the target tracking task in the lateral motion condition. The yaw only and centrifuge cueing conditions did not reveal any significant difference compared to the rumble only condition.

A number of explanations for the lack of the expected effects of motion in the present experiment exist. Additional tests indicate that the applied steering wheel disturbance had a fairly low frequency and low amplitude content from a motion perception threshold point of view, although subjects already indicated that the resulting displacements were large. A second explanation could be the information-rich preview display in the current experiment, which already provided excellent visual cues, especially in yaw direction. And, finally, differences in task instructions might have affected the results, since the subjects in [Zaa1] had to track a reference signal as aggressively as possible, while the present study required the subjects to drive as they would normally do, permitting them to ignore to the disturbances as long as they would remain between the lane markers. Further research will have to be performed to provide more insight.

From the data we can only conclude that the addition of motion did not improve performance. It is not possible to draw conclusions about the motion fidelity, or realism of the simulation, since we cannot compare the control activity and performance to data measured in a real car with unfiltered motion cues.

For this reason, we also had our subjects fill out a subjective rating scale during the experiment. All subjects indicated that it was difficult to assess the realism due to the presence of the steering wheel disturbance, which was much more present than in every-day driving. For that reason the fidelity of the ratings is low. Nevertheless the ratings indicated that the centrifuge and lateral track conditions were considered most realistic (average 5.9 and 5.8 out of 10), and the one-to-one yaw and rumble only conditions were less realistic (average 3.8 and 3.2 out of 10).

Based on the objective results, it is argued that the addition of motion during curve driving tasks in the presence of disturbances does not aid the driver in terms of lateral performance or control activity, and it appears only to influence the subjective realism.

Conclusions

A curve negotiation task at a prescribed and constant velocity was performed in the presence of external disturbances to investigate the effects of four different motion cueing algorithms on the control activity and performance.

Under the present experiment conditions, it can be concluded that none of the motion cueing conditions had a significant or large effect on the performance or control activity, neither in the target tracking task, as was expected, nor in the disturbance rejection task, which was unexpected.

The addition of motion only appeared to affect the subjective realism.

References

[All1] R. W. Allen, D. T. McRuer, J. R. Hogge, R. W. Humes, A. C. Stein, J. F. O'hanlon, R. T. Hennessy, G. R. Kelley, and G. V. Bailey, "Drivers' Visibility Requirements For Roadway Delineation, Volume I: Effects of Contrast and Configuration on Driver Performance and Behavior," Systems Technology, Inc., Tech. Rep. FHWA-RD-77-165, Nov. 1977.

[Dam1] H. J. Damveld, "A Cybernetic Approach to Assess the Longitudinal Handling Qualities of Aeroelastic Aircraft," Ph.D. dissertation, Delft University of Technology, Faculty of Aerospace Engineering, May 2009.

[Dam2] H. J. Damveld, D. A. Abbink, M. Mulder, M. Mulder, M. M. van Paassen, F. C. T. van der Helm, and R. J. A. W. Hosman, "Measuring the Contribution of the Neuromuscular System During a Pitch Control Task," in *Proceedings of the AIAA Modeling and Simulation Technologies Conference, Chicago, Illinois, Aug. 10-13, 2009*, no. AIAA-2009-5824. American Institute of Aeronautics and Astronautics, Aug. 2009.

[Dam3] H. J. Damveld, D. A. Abbink, M. Mulder, M. Mulder, M. M. van Paassen, F. C. T. van der Helm, and R. J. A. W. Hosman, "Identification of the Feedback Component of the Neuromuscular System in a Pitch Control Task," in *Proceedings of the AIAA Guidance, Navigation, and Control Conference 2 - 5 August 2010, Toronto, Ontario Canada*, M. Silvestro, Ed., no. AIAA 2010-7915, American Institute of Aeronautics and Astronautics. American Institute of Aeronautics and Astronautics, Aug. 2010, pp. 1–22.

[Dam4] H. J. Damveld, G. C. Beerens, M. M. van Paassen, and M. Mulder, "Design of Forcing Functions for the Identification of Human Control Behavior," Journal of Guidance, Control, and Dynamics, vol. 33, iss. 4, pp. 1064–1081, 2010.

[Gib1] J. J. Gibson, "What gives rise to the perception of motion?" Psychological Review, vol. 75, iss. 3, pp. 335–346, 1968.

[McR1] D. T. McRuer, R. W. Allen, D. H. Weir, and R. H. Klein, “New Results in Driver Steering Control Models,” *Human Factors: The Journal of the Human Factors and Ergonomics Society*, vol. 19, no. 4, pp. 381–397, Aug. 1977.

[Poo1] D. M. Pool, P. M. T. Zaal, H. J. Damveld, M. M. van Paassen, and M. Mulder, “Pilot Equalization in Manual Control of Aircraft Dynamics,” in *Proceedings of the 2009 IEEE International Conference on Systems, Man, and Cybernetics San Antonio, TX, USA - October 2009*, Institute of Electrical and Electronics Engineers. Institute of Electrical and Electronics Engineers, Oct. 2009, pp. 2480–2485.

[Rie1] P. Riekert and T. E. Schunck, "Zur Fahrmechanik des gummibereiften Kraftfahrzeugs," Archive of Applied Mechanics, vol. 11, iss. 3, pp. 210–224, 1940.

[Ste1] J. Steen, H. J. Damveld, R. Happee, M. M. van Paassen, and M. Mulder, “A Review of Visual Driver Models for System Identification Purposes,” in *Proceedings of the 2011 IEEE International Conference on Systems, Man, and Cybernetics Anchorage, AK, USA*, Oct. 2011.

[Val1] A. R. Valente Pais, M. Wentink, M. M. van Paassen, and M. Mulder, "Comparison of Three Motion Cueing Algorithms for Curve Driving in an Urban Environment," Presence: Teleoperators & Virtual Environments, vol. 18, iss. 3, pp. 200–221, 2009.

[Was1] R. J. Wasicko, D. T. McRuer, and R. E. Magdaleno, "Human Pilot Dynamic Response in Single-loop Systems with Compensatory and Pursuit Displays," Air Force Flight Dynamics Laboratory, AFFDL-TR-66-137, 1966.

[Wen1] M. Wentink, Valente Pais, R., Mayrhofer, M., Feenstra, P., Bles, W. (2008). First curve driving experiments in the Desdemona simulator. Proceedings of the Driving Simulation Conference Europe, Monaco, 183–192.

[Zaa1] P. M. T. Zaal, D. M. Pool, M. M. van Paassen, and M. Mulder, "Comparing Multimodal Pilot Pitch Control Behavior Between Simulated and Real Flight," in Proceedings of the AIAA Modeling and Simulation Technologies Conference, Portland, Oregon, Aug. 8-11, 2011

[Zaa2] P. M. T. Zaal, D. M. Pool, J. de Bruin, M. Mulder, and M. M. van Paassen, "Use of Pitch and Heave Motion Cues in a Pitch Control Task," Journal of Guidance, Control, and Dynamics, vol. 32, iss. 2, pp. 366–377, 2009.